ERRATA

NASA Technical Paper 3001

EVALUATION OF VARIOUS THRUST CALIBRATION TECHNIQUES
ON AN F404 ENGINE

Ronald J. Ray
April 1990

Title is incorrect. It should read "Evaluation of Various Thrust Calculation
Techniques on an F404 Engine." Please replace cover, title page, and Report
Documentation Page with the attached corrected pages.

Issue date: May 1990

Evaluation of Various Thrust Calibration Techniques on an F404 Engine

Ronald J. Ray

NASA

Evaluation of Various Thrust Calibration Techniques on an F404 Engine

Ronald J. Ray
Ames Research Center
Dryden Flight Research Facility
Edwards, California

CONTENTS

SUMMARY

In support of performance testing of the X-29A aircraft at the NASA Ames Research Center, Dryden Flight Research Facility, various thrust calculation techniques have been developed and evaluated for use on the F404-GE-400 engine (General Electric, Lynn, Massachusetts). The engine was thrust calibrated at the NASA Lewis Research Center's Propulsion System Laboratory. Results from these tests were used to correct the manufacturer's in-flight thrust program to more accurately calculate thrust for the specific test engine. Data from these tests were also used to develop an independent, simplified thrust calculation technique for real-time thrust calculation. Comparisons were also made to thrust values predicted by the engine specification model. Results indicate uninstalled gross thrust accuracies on the order of 1 to 4 percent for the various in-flight thrust methods. The various thrust calculations are described and their usage, uncertainty, and measured accuracies are explained. In addition, the advantages of a real-time thrust algorithm for flight test use and the importance of an accurate thrust calculation to the aircraft performance analysis are described. Finally, actual data obtained from flight tests are presented.

INTRODUCTION

The determination of in-flight thrust is important to any aircraft performance analysis. Because the direct measurement of thrust and drag in flight is not feasible, various methods have been devised to calculate thrust indirectly from the measurement of related engine parameters. There is no globally standard thrust calculation method because of the variety of engines, diversity of applications, and accuracy requirements.

A number of reports have been written on in-flight thrust calculation methodology and error assessment. Two of the more comprehensive references include AGARD (1979) and Society of Automotive Engineers (1986). The gas generator method of thrust calculation has been used on the XB-70 (Arnaiz and Schweikhard, 1970) and F-111 (Burcham, 1971) airplanes. A simplified gross thrust computing method, developed by Computing Devices Company (ComDev) of Ottawa, Ontario, Canada, has been evaluated on the F100 and J85 engines (Kurtenbach, 1979; Baer-Riedhart, 1982) and flown in a KC-135 aircraft (Hughes, 1981) and an F-15 aircraft (Kurtenbach and Burcham, 1981).

To evaluate and to compare various thrust calculation procedures, the NASA Ames Research Center, Dryden Flight Research Facility (Ames-Dryden) conducted a comprehensive study on the F404 engine in the X-29A forward-swept-wing advanced technology demonstrator airplane. The determination of thrust is particularly important for the X-29A airplane because many of its advanced technology features are designed to improve aircraft performance. This study has included a calibration of the flight engine at NASA Lewis (Burns and Kirchgessner, 1987), sensitivity studies (Hughes et al., 1985; Hamer and Alexander, 1978), and a flight evaluation on the X-29A aircraft including the application of four thrust calculation techniques.

The four thrust calculation techniques investigated include two variations of the engine manufacturer's in-flight thrust (IFT) program, the engine specification model, and an independent, simplified thrust technique for real-time thrust calculation. Two gas generator methods are used to calculate thrust in the IFT program: one is sensitive to nozzle area and pressure, while the other is sensitive to mass flow and temperature. ComDev's simplified method of calculating thrust has advantages over the traditional in-flight methods in that it requires much less instrumentation and computational resources. The engine specification model is a large computer model that predicts all the internal characteristics of the engine and its performance. The flight F404 engine was calibrated for thrust at the NASA Lewis Research Center's Propulsion System Laboratory (PSL). Data from these tests were used to correct the IFT program to more accurately calculate thrust of the specific engine and to develop the simplified thrust method.

The four thrust calculation techniques, their usage, advantages and disadvantages, and their predicted uncertainties and measured accuracies are described in this report. The altitude thrust calibration test and the general procedures used to calibrate the models are also described. Finally, examples of flight data on the X-29A aircraft and the effect of thrust accuracy on aircraft performance are presented.

NOMENCLATURE

AB	afterburner
AP	area-pressure thrust calculation method
$A8$	nozzle throat area, ft^2
a_x	longitudinal acceleration (body axis, positive-forward), g
a_z	normal acceleration (body axis, positive-up), g
C_D	aircraft drag coefficient
C_{FG}	gross thrust coefficient
C_i	influence coefficient
C_L	aircraft lift coefficient
ComDev	Computing Devices Company
D_{nozzle}	external nozzle drag, lb
D_{spill}	inlet spillage drag, lb
ECU	electronic control unit
F_{RAM}	ram drag, lb
FG	gross thrust, lb
FN	net thrust, lb
FNP	net propulsive thrust, lb
FSE	full-scale error, percent
FVG	fan inlet variable guide vanes
H	total enthalpy, BTU/lb
HPC	high-pressure compressor
$HPVG$	high-pressure compressor variable guide vanes
h_p, alt	pressure altitude, ft
IFT	in-flight thrust (program)
IRT	intermediate rated (maximum non-afterburning) thrust (PLA = 87°)
i	thrust incidence angle, deg
LPT	low-pressure turbine
M	Mach number
$N1$	fan rotor speed, rpm
$N2$	compressor rotor speed, rpm
PD	percent difference (accuracy), percent
PLA	power lever angle, deg
PSL	Propulsion System Laboratory (NASA Lewis Research Center)
p_{ref}	reference pressure, lb/in^2
p_s	static pressure, lb/in^2
p_t	total pressure, lb/in^2
q	dynamic pressure, lb/in^2
S	reference wing area, ft^2
SGTM	simplified gross thrust method
T_T	total temperature, °R
U	uncertainty, percent
V	velocity, ft/sec
W	engine airflow, lb/sec
WF	fuel flow, lb/hr
WT	mass flow-temperature thrust calculation method
wt	airplane weight, lb
α	angle of attack, deg
β	angle of sideslip, deg
Δ	difference
∂	partial derivative
σ	standard deviation

Subscripts:

$calc$	calculated
E	main engine (core)
I	ideal
$meas$	measured
P	pilot afterburner segment
$spec$	specification

F404 engine station identification numbers:

0	free stream
1	engine inlet face
3	high-pressure compressor discharge
4	combustor discharge
6	afterburner inlet
7	exhaust nozzle inlet
8	exhaust nozzle throat

2

9	exhaust nozzle discharge
25	high-pressure compressor inlet
558	low-pressure turbine discharge-measuring plane

AIRCRAFT DESCRIPTION

The X-29A advanced technology demonstrator is a single-seat, fighter-type aircraft incorporating several new technology concepts developed to enhance aircraft performance. The most notable aircraft feature is the forward-swept wing with a 29.3° leading-edge sweep and a thin, supercritical airfoil section. Graphite-epoxy composite materials are used to aeroelastically tailor the wing and inhibit wing structural divergence. Another notable feature of the aircraft is its active three-surface pitch control configuration, including wing flaperons, canards, and aft-mounted strake flaps. The canards act as a powerful lift and pitch moment generator. The aircraft's 35-percent negative static margin requires a high level of stability augmentation provided by a triple-redundant digital fly-by-wire flight control system.

The X-29A airplane is 48 ft long and has a wing span of 27 ft. The aircraft's F404 engine is mounted in the fuselage with two side-mounted fixed geometry inlets designed for both subsonic and transonic operation. Maximum aircraft takeoff gross weight is 17,800 lb with a 4000-lb fuel capacity. Additional information on the design of the X-29A aircraft can be found in Moore and Frei (1983).

ENGINE DESCRIPTION

The F404-GE-400 engine (General Electric, Lynn, Massachusetts) shown in figure 1 is a low-bypass, twin spool, augmented turbofan of the 16,000-lb thrust class. The engine incorporates a three-stage fan and a seven-stage high-pressure compressor, each driven by a single-stage turbine. Variable geometry is available on the fan inlet variable guide vanes (FVG) and on the high-pressure compressor variable guide vanes ($HPVG$). Bleed air extraction is provided at the seventh stage of the high-pressure compressor for environmental cooling control. The combustor is a through-flow annular type using atomizing fuel nozzles. The augmentor is fully modulating from minimum to maximum augmentation and uses fan discharge air and an augmentor liner to maintain a low

outer skin temperature on the engine. The hinged-flap, cam-linked exhaust nozzle is hydraulically actuated. An engine accessory gearbox is driven by the compressor spool. The gearbox powers the lubrication and scavenger oil pumps, variable exhaust nozzle power unit, generator, and both the main and afterburner fuel pumps. A schematic view of the F404-GE-400 engine with station designations is shown in figure 2.

The engine control system consists of the throttle, main fuel control, electric control unit, and afterburner fuel control. Throttle movement is mechanically transmitted to a power lever control. The power lever positions the main fuel control. Below the intermediate-rated thrust (IRT) power setting, compressor rotor speed ($N2$) is controlled by throttle movement and engine inlet total temperature (T_{T_1}) through the main fuel control. At IRT and above, fan rotor speed (N1) is controlled by the electronic control unit (ECU) as a function of T_{T_1}. The ECU senses engine and aircraft parameters, computes engine schedules, and maintains engine limits. The afterburner fuel control schedules fuel flow to the pilot spraybar and main spraybars. When the throttle is advanced to an afterburner setting, the afterburner ignitors are turned on, the exhaust nozzle opens slightly above the IRT position, the low-pressure turbine discharge total temperature (T_{T_5}) schedule is temporarily reset to a lower value, and afterburner pilot spraybar fuel flow and minimum main afterburner fuel flow begins. When afterburner light-off is detected, the ignitors are turned off, and the main afterburner fuel flow level increases to the level selected by the throttle position.

INSTRUMENTATION

The instrumentation mounted on the engine for the calculation of in-flight thrust is shown in figure 2 and listed in table 1. With the exception of the nozzle static pressures (p_{s_6} and p_{s_7}), this instrumentation was provided by the manufacturer as part of the F404 engine thrust instrumentation system. Volumetric flowmeters are used to measure fuel flows of the main engine core (WF_E), afterburner (WF_{AB}), and afterburner pilot (WF_{AB_P}). These meters were individually calibrated with the aircraft upstream fuel lines in place to simulate installation in the X-29A aircraft. Fuel temperatures are measured in both the core and afterburner fuel lines to permit conversion of volumetric values to mass flow.

The low-pressure turbine discharge total pressure ($p_{t_{5.8}}$) is measured by four 5-element total pressure rakes with all 20 elements individually measured and mathematically averaged. A single production $p_{t_{5.8}}$ probe is also used to measure pressure at this location. The exhaust nozzle throat area $A8$ is measured by an electric signal from a linear variable position transmitter. This system is calibrated to give the throat area in engineering units (in^2). Fan speed, fan variable guide vane positions, and T_{T_1} are all measured by electrical sensors. Compressor speed is also an electrical signal and is measured off the alternator. Compressor variable vane position and compressor discharge pressure (p_{s_3}) are both hydromechanical sensors.

To incorporate the ComDev simplified gross thrust method (SGTM), the afterburner liner was equipped with static pressure taps at stations 6 and 7. Accurate pressure, representative of conditions in the afterburner, is required for the ComDev method, and, therefore, four static pressures are measured at each station and mathematically averaged to obtain p_{s_6} and p_{s_7}. The SGTM also uses the 20-port $p_{t_{5.8}}$ pressure rakes. The $p_{t_{5.8}}$, p_{s_6}, and p_{s_7} pressures are measured by a 32-channel, ± 10 lb/in^2, differential transducer unit referenced to a spare p_{s_6} tap. The reference pressure is measured by an accurate absolute transducer. The 32-channel differential transducer is thermally controlled by a heater insulation blanket to maintain a constant temperature during flight. The unit was calibrated at this temperature to provide the best accuracy during flight. The average of the pressures at each rake is calculated by a software routine that also determines if individual pressures are within a specified tolerance of the average. Pressures outside the tolerance are omitted from the average. This ensures the highest quality measurement at each station even in the event of a broken or damaged pressure line.

Both the IFT program and SGTM require ambient static pressure (p_{s_0}) supplied by the aircraft air-data system. The IFT program also requires altitude (h_p) and Mach number (M) which are also supplied by the aircraft.

THRUST CALCULATION METHODS

In-Flight Thrust Program

The IFT program (General Electric, 1983) discussed in this report was developed by the General Electric Company for the U.S. Navy. The purpose of this program is to provide an accurate calculation of airflow and thrust for the F404 engine throughout the flight envelope.

In general, the IFT program treats the engine as a gas generator, modeling compressor, combustion, and turbine components to determine mass flow, pressure, and temperature at the exhaust nozzle. Internal flow-path measurements within the gas generator are used, together with mass-, momentum-, and energy-continuity principles, to calculate flow conditions at various stations within the engine and to predict overall engine performance (Society of Automotive Engineers, 1986). Engine-to-engine variations are accounted for by the actual measurement variations.

The IFT program uses two correlating methods, the area-pressure (AP) and the mass flow-temperature (WT) equations, for determining ideal gross thrust. The AP method is strongly dependent upon an accurate measurement of $A8$ and nozzle pressure ratio p_{t_8}/p_{s_0}. The WT procedure requires an accurate determination of mass flow and exhaust gas temperature and thus requires an accurate afterburner efficiency model. Detailed development of the gas generator methods for gross thrust calculation is given in AGARD (1979) and Burcham (1971).

The F404 IFT program was developed from an extensive test database from which the necessary thrust correlations and engine performance models were derived. This database was the result of six engine test phases at the Naval Air Propulsion Center altitude test facility where in excess of 1500 data points were gathered over the flight envelope. This extensive altitude database in conjunction with sea level test data produced an accurate understanding of engine behavior over the flight envelope necessary to develop the IFT program.

The gas generator model calculation and data flows are shown in figure 3. The arrows show the input and flow of data, and the blocks within the schematic illustrate calculations. The model uses a combination of theoretical values, component test data, and full-scale engine data to generate the relationships necessary for the analysis.

The aircraft inlet, engine fan-compressor, combustor-turbine, afterburner, and nozzle are modeled separately as shown (fig. 3). The inlet model uses inlet pressure recovery values estimated from wind

tunnel data along with altitude, Mach number, T_{T_1}, $N1$, and FVG to calculate inlet conditions and engine airflow. The energy rise across the fan and compressor is then modeled to determine airflow, temperature, and specific total enthalpy at the combustor entrance. The combustor and afterburner are modeled separately using an energy balance with fuel flows and $p_{t_{558}}$ as inputs. Ideal gross thrust (FG_I) is then calculated as shown in figure 3. The nozzle analysis uses the input values of $A8$ and p_{s_0} to calculate the gross thrust coefficient (C_{FG}) and multiplies FG_I by this value to obtain actual gross thrust (FG). The two gas generator methods use a common approach in determining engine flow parameters but differ in their schemes to correlate these parameters and correct FG_I to obtain the desired AP and WT values of FG. Finally, net thrust (FN) is calculated from gross thrust by subtracting the ram drag term (F_{RAM}). The ram drag or freestream momentum value is obtained by multiplying engine inlet airflow (W_1) by the free-stream velocity (V_0).

The FN value calculated by the IFT program accounts for installation effects of inlet internal performance, nozzle internal performance, bleed air extractions, and shaft power extractions. External forces are also present due to installation in the aircraft. The net propulsive force (FNP) accounts for these external forces by subtracting the inlet spillage and nozzle drag terms from FN. External propulsive drag terms are typically less than 1 to 3 percent of the net thrust value. They are dependent on aircraft and engine interactions and vary with power setting. Normally, these values are determined from wind tunnel tests using scaled models with scaled power systems. For the X-29A aircraft, these values were estimated.

Simplified Gross Thrust Method

The Computing Devices Company's SGTM computes jet engine gross thrust based on a one-dimensional analysis of flow in the engine afterburner and exhaust nozzle. Because this method requires little instrumentation and computational storage, it is easier to implement than the traditional gas generator methods, and, therefore, is useful for computing in-flight gross thrust in real time. A derivation of the equations in the SGTM algorithm is presented in Hughes (1981) and McDonald (1974). A flowchart of the algorithm is shown in figure 4.

The SGTM requires gas pressure measurements from three afterburner locations and free-stream static pressure to compute in-flight gross thrust. The three afterburner measurements are $p_{t_{558}}$, flameholder exit static pressure (p_{s_6}), and exhaust nozzle inlet static pressure (p_{s_7}). Calibration coefficients were determined during altitude testing at the NASA Lewis PSL facility. These coefficients are applied to the equations to correct for the effects of friction, mass transfer (leakage), three-dimensional effects, and the effect of the simplifying assumptions used in the theory. The algorithm analyzes the flow in the afterburner duct from the turbine exit (station 558) to the exhaust nozzle exit (station 9) and determines the total pressure at the nozzle inlet (p_{t_7}). The effective exhaust nozzle throat area is also computed. Gross thrust is then computed from p_{t_7}, the nozzle throat area, and p_{s_0}.

The Computing Devices Company has developed a net thrust algorithm based on F404 data collected during altitude testing at the PSL facility. This algorithm was developed for real-time application on the X-29A aircraft and uses the simplified approach demonstrated with the SGTM. Preliminary results are encouraging (Ray et al., 1988).

Specification Program

The manufacturer's specification model is a full aerothermal, steady-state performance program (General Electric, 1981). The simulation provides the values of a number of internal flow parameters for the engine as well as its overall performance. These parameters include airflow, gross and net thrust, and all the required input parameters for the IFT program. Inputs to the specification model include altitude, Mach number, power lever angle, and ambient temperature. The model was derived from actual test data and represents the operation of an average F404-GE-400 engine.

CALIBRATION TESTING

The specific F404 performance engine (S/N 215209) for the X-29A aircraft was calibrated for thrust and airflow at the NASA Lewis PSL facility from late 1985 through early 1986. The main objectives of this test were to tailor the IFT program to calculate more accurately the thrust of the specific test engine and to quantify the accuracy. Also, calibration data were needed to obtain the co-

efficients required to develop and evaluate the accuracy of the SGTM. Finally, an additional research objective was to evaluate the accuracy of the specification model using data gathered on the test engine.

Figure 5 shows the F404 engine installed in the PSL altitude test chamber. The engine was supported by an overhead mount coupled to the thrust bed. The thrust bed provided a calibrated load cell system for determining actual gross thrust. A bell-mouth inlet duct section was used and was specially instrumented for determining engine inlet mass flow. Inlet air temperature and pressure along with test chamber pressure were regulated to simulate proper altitude and Mach number conditions. The PSL facility is able to simulate various flight conditions by varying the flow conditions to the engine and the static pressure in the test chamber. This included varying ambient temperature of the air flowing to the engine so that the effects of an off-standard day could be determined. Over 150 test points were gathered at 11 flight conditions and at various power lever angle (PLA) settings.

The simulated flight conditions tested are presented in table 1. Engine power settings varied for each condition as shown. This matrix was chosen to represent the X-29A airplane's flight envelope and to concentrate on the two design points at 30,000 ft: Mach 0.9 and Mach 1.2. A general test procedure for each condition was to first establish the proper Mach number and altitude in the PSL test chamber. The engine was then allowed to stabilize at the test PLA setting for 5 min (2 min for afterburner PLA settings). Data were then recorded over 10- and 20-sec time periods. The data were time averaged, and statistical computations were made on the 20-sec-period data to verify stabilization of the recorded parameters. Data were also gathered by sequentially increasing and decreasing PLA to assess the presence of hysteresis in the throttle system. Burns and Kirchgessner (1987) give a detailed account of the calibration test and procedures.

The IFT program was calibrated by applying correction terms in a sequential manner to engine airflow, gross thrust, and net thrust for both the WT and AP thrust calculation methods. That is, first the airflow calibration was applied, then the gross thrust, and finally the net thrust. The calibration of airflow thus affects the calculation of gross and net thrust just as the calibration of gross thrust also affects the calculation of net thrust. Both the AP and WT gross thrust methods were calibrated independently.

Correlation parameters were determined by plotting the individual calibration parameters against those parameters expected, from engineering judgment, to be influential in the calculation of that term. The airflow calculation, for example, was sensitive to parameters such as fan speed, inlet pressure ratio (p_{t_1}/p_{s_1}), p_{s_3}, Mach number, and altitude. The percent difference between calculated and measured airflow was then plotted against each term along with calculated airflow itself. Polynomial curve fits were applied to determine which parameter showed the best correlation. The parameter with the best fit was determined using statistical methods, and the equation for the curve fit was then incorporated into the IFT program as a correction factor. More than one correction parameter could be used by repeating this process after implementing a correction. For airflow, inlet pressure ratio and p_{s_3} were determined to be the best correlating parameters.

UNCERTAINTY ANALYSIS

Since the exact thrust value of an engine cannot be measured directly in flight, it is important to estimate the uncertainty (U) of the calculated value. The uncertainty analysis can be applied to a thrust model before testing begins to evaluate its suitability for a flight experiment. It can also be useful in the posttest analysis of the data and can lead to a more thorough understanding of the results.

The term "uncertainty" in this report refers to the range of possible values of a parameter in a given test environment. For measurement data, it is based on estimations of instrumentation error (bias and random). For computed results, it is defined as the root-sum-square of the responses of the computation to each measurement uncertainty. The thrust uncertainty results presented in this report were predicted using estimated instrumentation accuracies and parameter measurement values obtained from the specification model.

Accuracy is defined as the deviation of values in relation to a defined reference, such as computed thrust compared with facility load cell measured thrust. The thrust and airflow accuracies presented in this report were derived using measured values from the calibra-

tion test as the reference. Both bias and random error values are presented.

The numbers for accuracy and uncertainty are valid only for the given test environment, but their relationship can be used to infer the accuracy of a computed parameter in an alternate test environment.

In-Flight Thrust Program Uncertainties

An analysis was conducted to determine the effect of the measurement accuracy that the input parameters have on the uncertainty of calculated thrust. Hughes et al. (1985) give a comprehensive discussion on this technique where a sensitivity analysis is used to predict the uncertainty of calculated thrust using the IFT program. The data presented in this section come from Conners (1989) using updated instrumentation accuracy values, which give improved results.

In general, the IFT program uncertainties were calculated as the root-sum-square of the uncertainties owing to the influence of each measurement uncertainty. Table 2 shows each input measurement parameter, its associated uncertainty, and range of value. The influence of each measurement was determined from a sensitivity analysis where first the baseline input conditions to the IFT program were determined for a flight condition using data obtained from the specification model. Each input variable then was independently changed by ± 1.0 percent and run again in the IFT program. Technically, the influence coefficient (C_i) is defined as the derivative of FG with respect to a change in influence or input parameter at the limit of zero change. This can be approximated as the percent change in thrust owing to a 1-percent change in a specified parameter:

$$C_i(\text{parameter}) = \Delta FG/FG \times 100 \text{ percent}$$
$$\text{for a } \pm 1\text{-percent } \Delta \text{ (parameter)}$$

In the sensitivity analysis, the C_i values were approximated linearly by calculating the effect of a -1.0- to 2.0-percent change. Figure 6 shows the percent change in gross thrust because of a change in the parameter $p_{t_{5ss}}$ for both the AP and WT thrust calculation methods. For the case shown, net thrust calculated using the AP method was more sensitive to a change in $p_{t_{5ss}}$ than was the WT method. The expected uncertainty of calculated thrust was determined by multiplying the expected accuracy for each of the

12 input parameters by its associated C_i value and by taking a root-sum-square of all the parameters. The equation used in determining the uncertainty in gross thrust (U_{FG}) was

$$U_{FG} =$$

$$\sqrt{[(C_{i_{ALT}} \times U_{ALT})^2 + (C_{i_M} \times U_M)^2 + \ldots]}$$

This procedure was used to determine the gross and net thrust uncertainty for both calculation methods over a range of six Mach number and altitude conditions for PLA settings from flight idle (30°) to maximum power (130°).

Figure 7 shows the results of the uncertainty analysis for the six simulated flight conditions. The gross thrust results indicate the WT method generally is superior to the AP method. For the WT method (fig. 7(a)), uncertainty decreases as PLA increases from 30° to intermediate power (87°). At IRT, gross thrust uncertainty for the WT method $U_{FG_{WT}}$ varies from 1.4 to 3.1 percent as a function of flight condition. Note the value of $U_{FG_{WT}}$ increases as PLA advances above IRT because of the addition of afterburner fuel flow WF_{AB} and its relatively large uncertainty (at low WF_{AB} values) and relatively large value of C_i, particularly at the middle afterburner power settings (PLA = 109°). The $U_{FG_{WT}}$ decreases above 109° PLA to a range of 1.0 to 2.2 percent. This decrease primarily is because of the decrease in WF_{AB} uncertainty. In comparison, the uncertainty in gross thrust for the AP method $U_{FG_{AP}}$ (fig. 7(b)) continually decreases above IRT. Its uncertainty at IRT varies from 4.0 to 5.3 percent, depending on the flight condition. At maximum power, $U_{FG_{AP}}$ ranges from 2.5 to 3.2 percent. Although the results show higher gross thrust uncertainties with the AP method, the method also shows less variation in uncertainty owing to changes in flight conditions. This holds true for all PLA values above 70°, indicating $U_{FG_{AP}}$ is less sensitive to variations in flight conditions than $U_{FG_{WT}}$.

The large uncertainty values at low PLA settings in part are owing to the large values of parameter uncertainty. Most parameter accuracies are based on the manufacturer's full-scale accuracy which in absolute terms is constant. As a parameter value decreases, its expected percent accuracy worsens. Low thrust values also tend to increase the individual C_i values, compounding the problem. Thus, the combination of large

7

C_i values and large input parameter uncertainties cause large uncertainty results at low PLA values. Actually, the absolute thrust uncertainty value, in pounds, may in fact decrease as PLA decreases even though its percent value increases.

The uncertainty in net thrust U_{FN} (figs. 7(c) and 7(d)) includes the effects of the gross thrust and the ram drag terms. Because both gross thrust methods use the same F_{RAM} value, one might expect the same difference between gross and net thrust uncertainties. However, because of the airflow term that appears both in the FG_{WT} and F_{RAM} calculations, a partial cancellation of the effect of this parameter's uncertainty occurs in the WT method. Thus, the WT method shows less overall increase in net thrust uncertainty compared to gross thrust uncertainty than with the AP method.

The uncertainty in net thrust results for the WT method is generally between 2 and 5 percent for PLA values above 70°, except for the 40,000 ft and Mach 0.8 condition where it approaches 8.0 percent at 109° PLA. In general, the uncertainty of the WT method $U_{FN_{WT}}$ increases with increasing altitude and decreases with increasing Mach number (fig. 7(c)). The uncertainty of the AP method $U_{FN_{AP}}$ varies from 4.0 to 10.5 percent for PLA values above 70° (fig. 7(d)). As in the WT method, $U_{FN_{AP}}$ generally increases with increasing altitude. Unlike the WT method, $U_{FN_{AP}}$ increases with increasing Mach number. It is interesting to note that the $U_{FN_{AP}}$ results are much more sensitive to variations in flight conditions than the $U_{FG_{AP}}$ results. In comparison, the $U_{FN_{WT}}$ results show the same sensitivity when compared to the gross thrust results. The data also show both methods are unusable at very low PLA settings owing to large uncertainties.

Simplified Gross Thrust Method Uncertainties

A sensitivity analysis was conducted to determine the amount that computed SGTM thrust changes with a change in each of the measured parameters. Uncertainties in instrumentation and their effect on calculated SGTM thrust are summarized in table 3. The sensitivity analysis produced influence coefficients for each parameter, which were multiplied by the expected error of the parameter to determine the expected error in SGTM-computed thrust resulting from measurement errors. Figure 8 shows the sensitivity of the SGTM

due to pressure measurement errors for various PLA settings at 30,000 ft and Mach 0.9. These results show that the SGTM is more sensitive at low PLA settings than at high settings, and that the algorithm is most sensitive to the p_{s7} measurement.

An uncertainty analysis was made using the results of the sensitivity study, the uncertainty of the in-flight instrumentation, and the estimated SGTM model error (Hamer and Alexander, 1978). Table 4 shows a sample tabulation of SGTM uncertainty for the 30,000 ft and Mach 0.9 condition at an IRT. The results of the uncertainty analysis for three power settings at 10 flight conditions are summarized in table 5, which indicates a slight reduction in predicted uncertainty as Mach number increases. The results are also shown in figure 9 for various flight conditions and PLA settings, indicating a decrease in the predicted uncertainty as PLA increases. The total uncertainty of in-flight SGTM gross thrust is better than ±2.6 percent of the reading for all conditions at a power setting of 70° PLA. At IRT, the gross thrust uncertainty is better than ±1.8 percent for all Mach and altitude conditions. At maximum afterburner, it is better than ±1.1 percent. At the aircraft design point of Mach 0.9 and 30,000 ft altitude, total uncertainty is ±1.5 percent at IRT and ±1.1 percent at maximum power.

ACCURACY OF METHODS

The accuracy of the IFT program, SGTM, and specification models were determined by calculating the percent difference in calculated thrust as compared to measured thrust using data gathered during the calibration tests:

$$PD_{FG} = [(FG_{CALC} - FG_{MEAS})/FG_{MEAS}] \times 100 \, \text{percent}$$

Because the data used in the calculation of gross thrust for the different calculation procedures come from the same instrumentation and the same test runs, their values are directly comparable. Figure 10 shows the gross thrust accuracy of the WT and AP methods from the IFT program after calibration, the ComDev SGTM, and the specification model plotted against facility-measured gross thrust. All four methods show a tendency to decrease in accuracy at low thrust values.

This corresponds to the predicted uncertainty for each calculated gross thrust method and with the uncertainty in measured gross thrust. The uncertainty in measured gross thrust improves as thrust increases. The WT method (fig. 10(a)) indicates the best overall accuracy, although the AP method (fig. 10(b)) is better below 5,000 lb measured thrust. The ComDev SGTM (fig. 10(c)) also shows good thrust accuracies, while the accuracy of predicted thrust from the specification model (fig. 11) is almost an order of magnitude worse than the other methods (note difference in scale), particularly at low thrust values.

The accuracy of the four gross thrust methods for various PLA settings is summarized in figure 12 and table 6. Bias values represent the average accuracy of each sample. Sigma (σ) values represent the standard deviation of the sample from the bias value and indicate data scatter. Statistically, 95 percent of the data sample will fall within ±2 standard deviations (±2 σ) of the bias if the data follow a normal distribution. Calibration of the IFT program and the SGTM has greatly reduced the bias values as shown in table 6. The accuracies of gross thrust for the IFT program as well as the SGTM were all less than 2 percent for the PLA range from 40° to 130°. For this same PLA range, the WT method displayed the best ±2 σ accuracy value at 1.12 percent followed by the AP method at 1.28 percent and the SGTM at 1.80 percent. The accuracy of the specification model, on the other hand, was 8.74 percent with a −1.30-percent bias for this PLA range. This result is somewhat expected since the specification model was not calibrated. These results clearly demonstrate that highly accurate in-flight gross thrust calculations are available and are being used on the X-29A aircraft.

The results confirm that WT is the most accurate of the methods evaluated. However, they also show the AP method to be more accurate than the SGTM at and below IRT, as shown in figure 12(a). On the other hand, the SGTM is slightly more accurate than the AP method during afterburner operation (fig. 12(b)). The accuracy results of the AP method were much better than those predicted by the uncertainty analysis. One reason for the improved accuracy is the use of calibration data to correct this method. Calibrating the AP method resulted in an improvement of over 1 percent in its measured accuracy.

THRUST EFFECTS ON AIRCRAFT PERFORMANCE COMPUTATION

The determination of total airplane lift and drag in flight is necessary to analyze the performance characteristics of an airplane and to compare with the available wind tunnel model data for that airplane. The method used to determine lift and drag for the X-29A airplane is the accelerometer method. This method has commonly been used for a number of years because it permits a complete coverage of the Mach number and angle-of-attack capabilities of an airplane. Beeler et al. (1956) discuss the accelerometer method in more detail; in addition, Saltzman and Ayers (1982) survey a wide variety of aircraft that have used the accelerometer method.

The determination of lift and drag by the accelerometer method requires the following parameters: body-axis longitudinal acceleration (a_x); body-axis normal acceleration (a_z); angle of attack (α); dynamic pressure (q); airplane weight (wt); and FG and FNP. The equations used here for lift coefficient (C_L) and drag coefficient (C_D) assume a symmetric maneuver ($\beta = 0°$) and are

$$C_L = [W(a_x \sin \alpha + a_z \cos \alpha) - FG \sin(\alpha + i)]/q \cdot S$$

$$C_D = [FNP - W(a_x \cos \alpha + a_z \sin \alpha)]/q \cdot S$$

where,

FNP	$= FG \cos(\alpha + i) - F_{RAM} - D_{spill} - D_{nozzle}$
i	= thrust incidence angle, deg (0° for the X-29A aircraft)
D_{spill}	= inlet spillage drag, lb
D_{nozzle}	= external nozzle drag, lb

The expressions relating the uncertainty in C_L and C_D to the variation of thrust were obtained by taking the partial derivatives of each equation with respect to FN and FG. From the above equation, it is evident that a relationship exists between FN and FG. However, for simplicity, the errors caused by FN and FG

9

are treated as being independent, and the error caused by F_{RAM} is assumed to be included in the error estimate for FN. The resulting equations for the incremental errors in C_L and C_D with respect to FG and FN are

$$\partial C_L = \partial FG[-\sin(\alpha + i)]/q \cdot S$$
$$\partial C_D = \partial FN[\cos(\alpha + i)]/q \cdot S$$

The uncertainties of C_L and C_D due to thrust are determined by dividing ∂C_L by C_L and ∂C_D by C_D and multiplying by 100 percent. Powers (1985) discussed this method in detail and used this technique to calculate the uncertainty in lift and drag as a result of thrust for the X-29A airplane. The individual parameters used in this analysis were obtained from an X-29A simulation model. The results of this study show at $\alpha = 0°$, that the uncertainty in C_D because of the uncertainty in thrust is at most equal to the uncertainty in FN; that is, a 1-percent uncertainty in FN can result in a 1-percent uncertainty in C_D. As angle of attack increases or decreases from zero, the thrust uncertainty effect decreases because of the $\cos \alpha$ term. Thrust uncertainty has little effect on C_L uncertainty as a result of the $\sin \alpha$ term.

REAL-TIME THRUST

Because of the relative small size of the ComDev SGTM algorithm, it has obvious computational advantages over the more complex IFT and specification programs. To evaluate these advantages, a study was made on an ELXSI system 6400 computer (ELXSI, San Jose, California) to determine the memory requirements and computation time required to run an equal number of data points. The results were standardized to the IFT values and are shown in table 7. The SGTM required less than 10 percent of the memory storage requirements of the IFT program. It also computed the same 131 data points in 2.2 percent of the computational time the IFT program required. These numbers reflect the time required for data computation only and do not include the time required to process the output of the results. Because of the computational advantages of the ComDev method and its comparable accuracy to the IFT program, it has been selected for real-time thrust monitoring and calculation of in-flight performance on the X-29A project. Ray et al. (1988) describe the real-time performance system in detail for the X-29A airplane.

Figure 13 shows the real-time performance data system for the X-29A airplane. Data from the aircraft and engine are measured onboard the X-29A aircraft and transmitted by way of a multiplex signal to a ground-based receiver. After demultiplexing the signal, the data are passed to the real-time computer where the SGTM software calculates thrust, and a performance routine calculates aircraft lift and drag. These values are then sent to the proper display device in the control room.

COMPARISON OF METHODS DURING FLIGHT TESTS

A comparison of the gross thrust calculated by the various methods during flight is shown in figure 14. These data were gathered during performance flight testing of the X-29A aircraft. The results indicate good agreement between the methods for both the IRT (fig. 14(a)) and the maximum power (fig. 14(b)) accelerations presented. The WT method tends to calculate slightly higher thrust values than the AP and real-time methods (SGTM). Also, the WT method slightly diverges from the other two in-flight methods as Mach increases. The percent difference between methods is generally 1 to 5 percent. These values are within the predicted in-flight thrust uncertainties (methods summed together) presented in this report. As with the uncertainty predictions, the results show better agreement between methods for the maximum power case than for the IRT case.

Predicted test-day gross thrust, calculated by the specification program, is also presented for comparison in figure 14. The specification values tend to be generally higher than values from the other methods. This may be attributed to such things as the model error or uncertainty in the specification program, the uncertainty in various in-flight thrust calculation methods, the actual engine performance not being nominal (the specification program is not calibrated), and the lack of engine stabilization during the test manuever. In any case, the differences are small and indicate that reasonable thrust values are being calculated in flight.

These results help to validate the calibration of the various models and give confidence to their accuracies. They also show the real-time thrust method SGTM calculates similar results when compared to the postflight IFT methods. Additional comparisons can be found

10

in Hughes (1981) for data obtained on a KC-135 airplane and in Kurtenback and Burcham (1981) for data obtained on an F-15 airplane.

CONCLUDING REMARKS

Four methods of calculating thrust on an F404 engine have been discussed. These methods include the two gas generator techniques calculated by the in-flight thrust program: the mass flow-temperature method, and the area-pressure method used in postflight analysis of flight test data. The other methods are the predicted thrust values calculated by the engine specification model, and a simplified gross thrust method developed by the Computing Devices Company.

Four techniques have been evaluated with the following results:

1. An uncertainty analysis of the various in-flight thrust methods was made based on instrumentation accuracies. Results show the mass flow-temperature method with the lowest uncertainty followed by the simplified gross thrust and area-pressure methods.

2. An engine calibration test was performed at NASA Lewis Research Center's Propulsion System Laboratory altitude facility to calibrate the various thrust methods for more accurate calculation of thrust. Measured thrust data obtained from the calibration test were used to determine the accuracy of the various models. For a power lever angle range of 40° to 130°, results show the mass flow-temperature method to be the most accurate (± 1.12 percent), followed by the area-pressure thrust calculation method (± 1.28 percent), then the simplified gross thrust method (± 1.80 percent). Calibration removed most of the bias in each method. For the same power lever angle range, the uncalibrated specification method ac-

curacy was measured to be only ± 8.74 percent about a -1.30-percent bias.

3. The effects of thrust uncertainty on the calculation of aircraft performance uncertainty were examined. Thrust effects on drag at most are one-to-one. That is, a 1-percent uncertainty in the thrust calculation can cause a 1-percent error in aircraft drag coefficient. The effects of thrust uncertainty on calculated aircraft lift coefficient are much smaller.

4. An evaluation of the various methods shows the Computing Devices Company's simplified gross thrust method requires significantly less instrumentation and computational requirements than the in-flight thrust program. For this reason, it was chosen for use on the X-29A airplane for real-time thrust monitoring and performance calculation.

5. Data obtained during flight test of the X-29A aircraft show good agreement between the various thrust methods. The differences between methods were generally within their predicted uncertainty, giving confidence to the results. This confirms that the calibration curves obtained from calibration test data were reasonable.

Finally, highly accurate thrust calculations are available and are being used in support of the X-29A project. The information documented in this report will help flight engineers assess the aircraft's in-flight performance.

Ames Research Center
Dryden Flight Research Facility
National Aeronautics and Space Administration
Edwards, California, June 21, 1988

REFERENCES

AGARD, *Guide to In-Flight Thrust Measurement of Turbojets and Fan Engines*, AGARDograph no. 237, Jan. 1979.

Arnaiz, Henry H., and William G. Schweikhard, *Validation of the Gas Generator Method of Calculating Jet-Engine Thrust and Evaluation of XB-70-1 Airplane Engine Performance at Ground Static Conditions*, NASA TN D-7028, 1970.

Baer-Riedhart, Jennifer I., "Evaluation of a Simplified Gross Thrust Calculation Method for a J85-21 Afterburning Turbojet Engine in an Altitude Facility," AIAA 82-1044, 1982.

Beeler, De E., Donald R. Bellman, and Edwin J. Saltzman, *Flight Techniques for Determining Airplane Drag at High Mach Numbers*, NACA TN D-3821, 1956.

Burcham, Frank W., Jr., *An Investigation of Two Variations of the Gas Generator Method To Calculate the Thrust of the Afterburning Turbofan Engines Installed in an F-111A Airplane*, NASA TN D-6297, 1971.

Burns, Maureen E., and Thomas A. Kirchgessner, *Airflow Calibration and Exhaust Pressure/Temperature Survey of an F-404, S/N 215-209, Turbofan Engine*, NASA TM-100159, 1987.

Conners, T., "Measurement Effects on the Calculation of In-Flight Thrust for an F404 Turbofan Engine," AIAA 89-2364, 1989. Also available as NASA TM-4140, 1989.

General Electric, "F404-GE-400 Engine Specification Model," G.E. program no. 80031A(U), General Electric Co., Aug. 1981.

General Electric, "F404-GE-400 Engine In-flight Thrust Calculation Program," G.E. program no. 83112, General Electric Co., Aug. 1983.

Hamer, M.J., and R.I. Alexander, *Algorithm Development and System Error Analysis for Extension of Thrust Computing System Technology to the F100 Engine*, R80312/FR, Computing Devices Company, Ottawa, Canada, 1978.

Hughes, Donald L., *Comparison of Three Thrust Calculation Methods Using In-Flight Thrust Data*, NASA TM-81360, 1981.

Hughes, Donald L., Ronald J. Ray, and James T. Walton, "Net Thrust Calculation Sensitivity of an Afterburning Turbofan Engine to Variations in Input Parameters," AIAA 85-4041, 1985.

Kurtenbach, Frank J., *Evaluation of a Simplified Gross Thrust Calculation Technique Using Two Prototype F100 Turbofan Engines in an Altitude Facility*, NASA TP-1482, 1979.

Kurtenbach, Frank J., and Frank W. Burcham, Jr., *Flight Evaluation of a Simplified Gross Thrust Calculation Technique Using an F100 Turbofan Engine in an F-15 Airplane*, NASA TP-1782, 1981.

McDonald, G.B., *Theory and Design of an Airborne Thrust Computing System*, H036/119/FR/IV, Computing Devices Company, Ottawa, Canada, Aug. 1974.

Moore M., and D. Frei, "X-29 Forward-Swept Wing Aerodynamic Overview," AIAA 83-1834, 1983.

Powers, Sheryll Goecke, *Predicted X-29A Lift and Drag Coefficient Uncertainties Caused by Errors in Selected Parameters*, NASA TM-86747, 1985.

Ray, R.J., J.W. Hicks, and R.I. Alexander, *Development of a Real-Time Aeroperformance Analysis Technique for the X-29A Advanced Technology Demonstrator*, NASA TM-100432, 1988.

Saltzman, Edwin J., and Theodore G. Ayers, "Review of Flight-to-Wind-Tunnel Drag Correlation," *J. of Aircraft*, vol. 19, no. 10, Oct. 1982, pp. 801–811.

Society of Automotive Engineers, *In-Flight Thrust Determination and Uncertainty*, SAE SP-674, 1986.

Table 1. Thrust calibration test points.

h_p, ft	Mach	Flight idle	N2, percent				Min. IRT	AB	PLA, deg			Max. AB
			80	85	90	95	IRT	AB	100	110	120	AB
10,000	0.4	X*	X	—	X	—	X	—	—	—	X	—
	0.8	X	X	—	X	X	X	X	X	X	X	—
20,000	0.6	X	X	—	X	—	X	X	—	X	—	X
24,000	0.4	—	X	—	X	—	X	X	—	X	—	X
	0.9	—	—	—	—	—	X	X	—	X	—	X
30,000	0.5	X	—	X	—	X	X	—	X	—	—	X
	0.9	X	—	X	X	X	X	X	X	X	X	X
	1.2	X	X	—	—	—	X	—	X	—	—	X
40,000	0.8	X	—	—	X	—	X	X	—	X	—	X
	1.6	X	X	—	—	—	X	X	—	X	—	X
45,000	1.8	—	—	—	—	—	X	—	—	—	—	X

*X indicates test point at simulated flight condition.

Table 2. Measurement ranges and uncertainties of various thrust input parameters.

Parameter	No. of sensors	Range	Uncertainty, percent of full-scale	Methods using parameter (X = used)		
				IFT model	SGTM	Specification model
h_p*	1	$0 - 60,000$ ft	± 0.1	X	—	X
$A8$	1	$220 - 540$ in^2	± 2.0	X	—	—
FVG	1	$0 - 55°$	± 2.0	X	—	—
$HPVG$	1	$-5 - +55°$	± 2.0	X	—	—
M*	1	$0 - 2.0$	± 0.25	X	—	X
$N1$	1	$0 - 13,270$ rpm	± 1.0	X	—	—
PLA	1	$0 - 130°$	± 2.0	X	—	X
p_{s0}	1	$0 - 15$ lb/in^2	± 0.2	X	X	—
p_{s3}	1	$0 - 500$ lb/in^2	± 0.1	X	—	—
$p_{s6} - p_{ref}$	8	$-10 - +10$ lb/in^2	± 0.25	—	X	—
$p_{s7} - p_{ref}$	4	$-10 - +10$ lb/in^2	± 0.25	—	X	—
$p_{t558} - p_{ref}$	20	$-10 - +10$ lb/in^2	± 0.25	X	X	—
$p_{ref} (p_{s6})$	1	$0 - 60$ lb/in^2	± 0.1	X	X	—
T_{T1}	1	$-60 - 400°$F	± 1.0	X	—	—
WF_{AB}	1	$0 - 30,000$ lb/hr	± 2.0	X	—	—
WF_{ABP}	1	$0 - 1,500$ lb/hr	± 2.0	X	—	—
WF_E	1	$0 - 12,000$ lb/hr	± 2.0	X	—	—

*Estimated from calculation.

Table 3. Change in computed SGTM gross thrust (percent of reading) resulting from pressure transducer errors.

(a) Pressure measurement error.

Transducer	Full-scale value, lb/in²	FSE, percent	FSE, lb/in²	No. of transducers	Net error, lb/in²
p_{a0}	19	0.2500	0.0475	1	0.0475
p_{ref}	50	0.0160	0.0080	1	0.0080
$p_{ts8} - p_{ref}$	20	0.1640	0.0328	20	0.0073
$p_{a6} - p_{ref}$	20	0.1640	0.0328	4	0.0164
$p_{a7} - p_{ref}$	20	0.1640	0.0328	4	0.0164

(b) Error of SGTM gross thrust, percent of reading.

		h_p, ft									
		10,000			24,000		30,000			40,000		45,000
		Mach										
PLA, deg	Transducer	0.3	0.6	0.8	0.3	0.9	0.5	0.9	1.2	0.8	1.5	1.8
70	p_{a0}	---	−0.309	−0.155	−0.364	---	---	−0.311	---	−0.583	---	---
	p_{ref}	---	0.052	0.018	0.061	---	---	0.032	---	0.074	---	---
	$p_{ts8} - p_{ref}$	---	0.054	0.101	0.052	---	---	0.220	---	0.072	---	---
	$p_{a6} - p_{ref}$	---	−0.211	0.113	−0.255	---	---	0.242	---	−0.380	---	---
	$p_{a7} - p_{ref}$	---	0.179	−0.306	0.245	---	---	−0.688	---	0.332	---	---
87	p_{a0}	−0.158	−0.188	−0.129	−0.249	−0.170	−0.292	−0.224	−0.195	−0.420	−0.307	−0.441
	p_{ref}	0.018	0.019	0.014	0.027	0.015	0.028	0.018	0.016	0.034	0.019	0.023
	$p_{ts8} - p_{ref}$	0.124	0.170	0.088	0.226	0.160	0.294	0.208	0.129	0.359	0.132	0.179
	$p_{a6} - p_{ref}$	0.137	−0.186	−0.099	0.241	0.173	0.310	0.218	0.141	0.373	0.144	0.181
	$p_{a7} - p_{ref}$	−0.385	−0.541	−0.271	−0.719	−0.512	−0.958	−0.667	−0.404	−1.170	−0.406	−0.542
130	p_{a0}	---	−0.242	---	−0.323	−0.205	−0.362	−0.251	−0.207	−0.441	−0.257	−0.326
	p_{ref}	---	0.025	---	0.033	0.019	0.036	0.023	0.019	0.041	0.023	0.027
	$p_{ts8} - p_{ref}$	---	0.068	---	0.094	0.061	0.112	0.081	0.051	0.141	0.050	0.067
	$p_{a6} - p_{ref}$	---	0.032	---	0.043	0.028	0.051	0.037	0.024	0.064	0.024	0.028
	$p_{a7} - p_{ref}$	---	−0.135	---	−0.185	−0.126	−0.231	−0.171	−0.101	−0.299	−0.089	−0.122

Table 4. Computation of SGTM gross thrust uncertainty
at Mach 0.9, 30,000 ft altitude, IRT.

	Error in SGTM gross thrust (percent of reading)
$[FG_{SGTM} - FG_{meas} \times 100]/FG_{meas}$	1.453*
Number of points defining bias, σ, and U	48
NASA Lewis thrust error	0.417
NASA Lewis pressure error	0.557
Observed SGTM system error	1.276
SGTM model error	1.274
Calibration bias limit	0.184
NASA Ames-Dryden pressure error	0.732
Total SGTM in-flight uncertainty, $U_{FG_{SGTM}}$	1.480

*Observed accuracy at NASA Lewis PSL.

Table 5. Total uncertainty of SGTM gross thrust, percent of reading.

	h_p, ft										
	10,000		20,000	24,000		30,000			40,000		45,000
	Mach										
PLA, deg	0.3	0.8	0.6	0.3	0.9	0.5	0.9	1.2	0.8	1.5	1.8
70	---	2.518	2.511	2.521	---	---	2.608	---	2.547	---	---
87	1.356	1.322	1.419	1.511	1.405	1.660	1.480	1.362	1.815	1.364	1.419
130	---	---	1.046	1.056	1.044	1.067	1.052	1.041	1.088	1.039	1.044

Table 6. Comparison of gross thrust calculation methods
based on Lewis calibration data.

PLA, deg	No. of points	FG_{SGTM} Bias, %	2σ, %	FG_{WT} method Bias, %	2σ, %	FG_{AP} method Bias, %	2σ, %	FG_{spec} method Bias, %	2σ, %
31	19	*	*	−0.05	4.22	1.72	10.04	−29.69	23.69
40–87	81	−0.04	2.14	0.04	1.33	−0.16	1.29	−0.01	11.57
90–130	50	0.10	1.04	0.01	0.68	0.12	1.18	−2.09	4.22
40–130	131	−0.07	1.80	0.03	1.12	−0.05	1.28	−1.30	8.74

*The minimum PLA for the ComDev gross thrust method is 40°.

Table values represent the percent difference between calculated and measured values; for the ComDev method, bias and 2σ were calculated using $\frac{FG_{SGTM} - FG_{meas}}{FG_{meas}} \times 100$.

Table 7. Comparison of thrust computational requirements
on an ELXSI computer.

Method	Memory requirements, percent of IFT model	Computational time, percent of IFT model	Application
ComDev SGTM	9.50	2.21	Real time
G.E. IFT program	100.00	100.00	Postflight
G.E. specification program	1745.50	248.35	Predictions
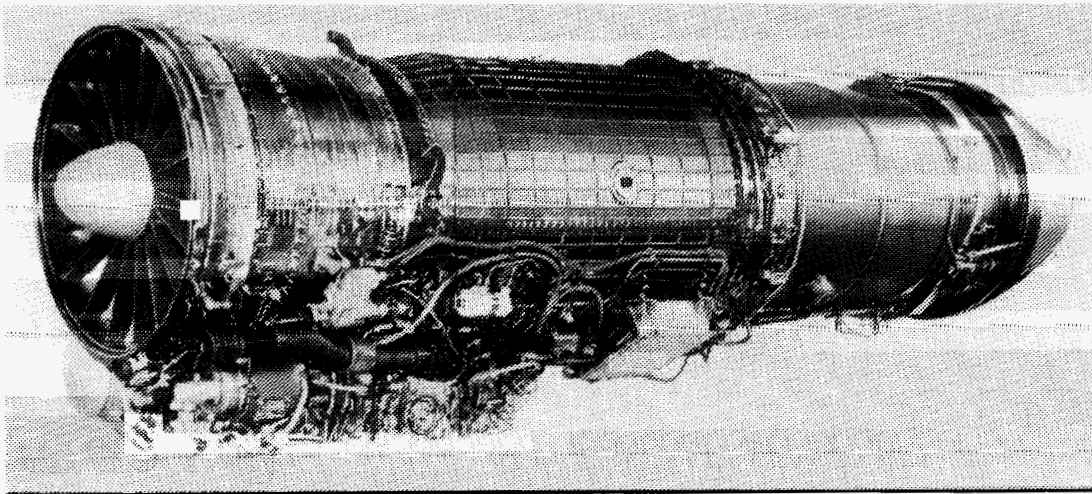
ECN 33131-001

Figure 1. General Electric F404-GE-400 afterburning turbofan engine.

16
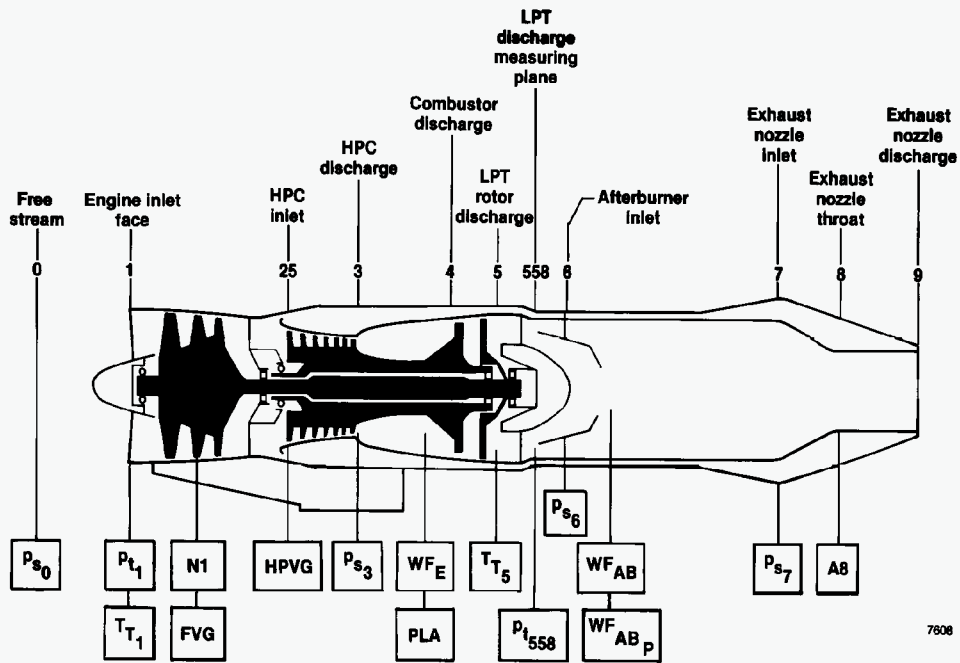
Figure 2. Engine station and sensor locations.
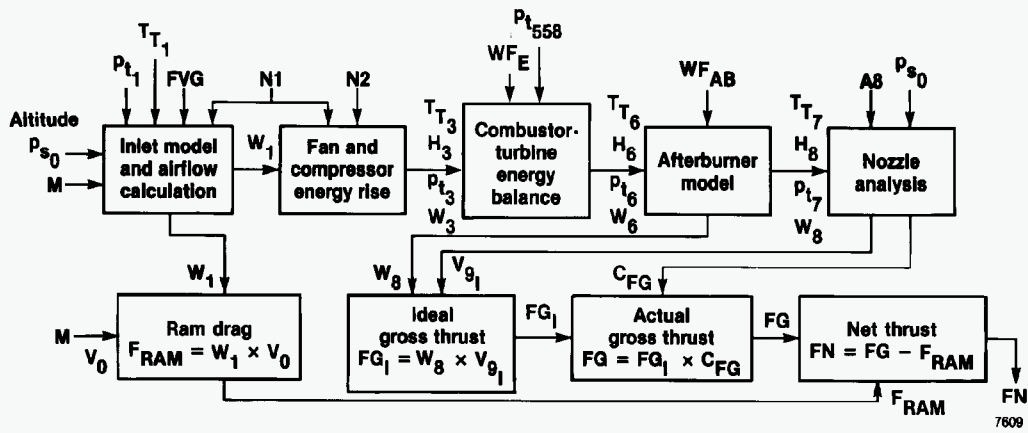
Figure 3. F404 in-flight thrust flowchart.

17
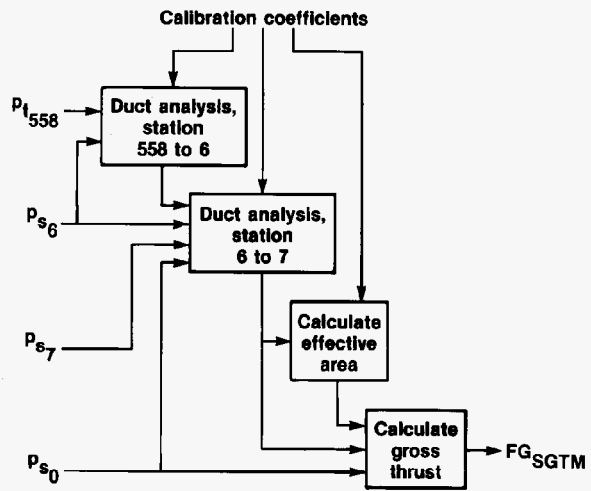
Figure 4. Flowchart for the ComDev SGTM.
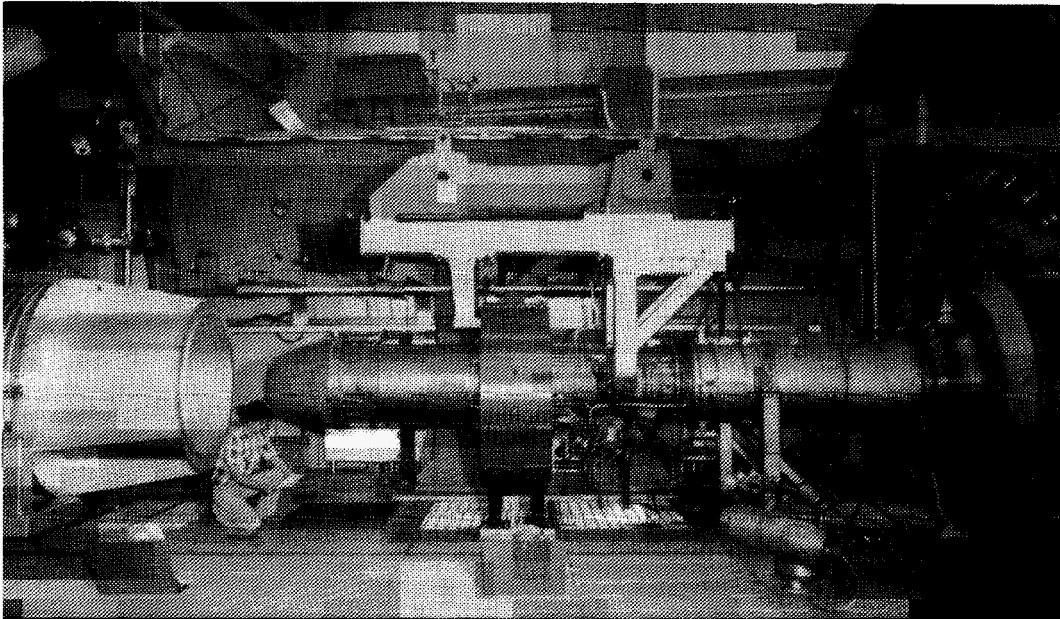
ECN 33370-001

Figure 5. Engine installation in the test chamber.

18
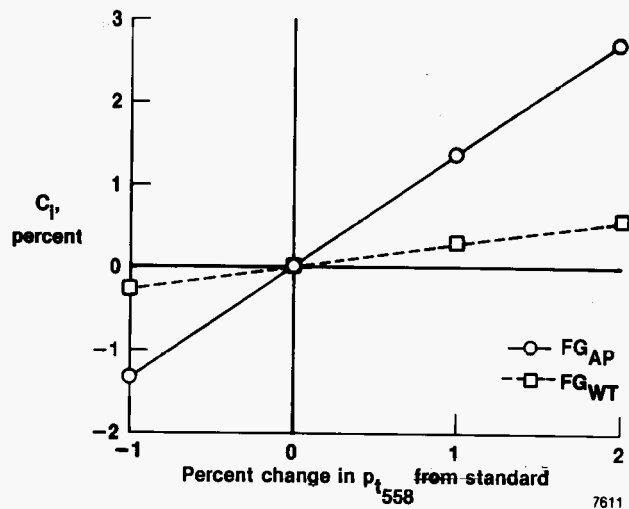
Figure 6. Comparison of FG_{AP} and FG_{WT} for a -1.0-percent to a 2.0-percent change in $p_{t_{558}}$ at Mach 0.9 and a 30,000-ft altitude at intermediate power.
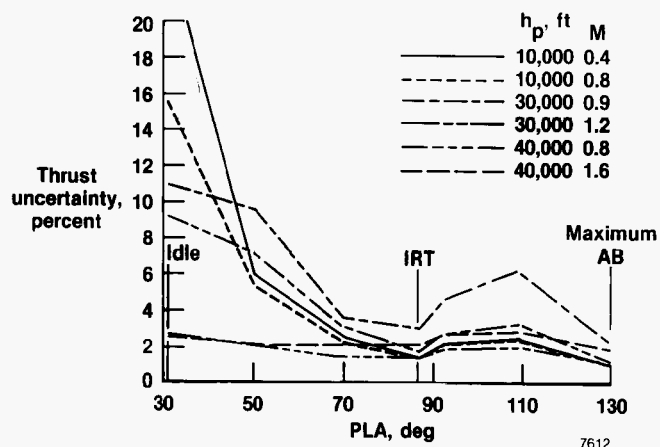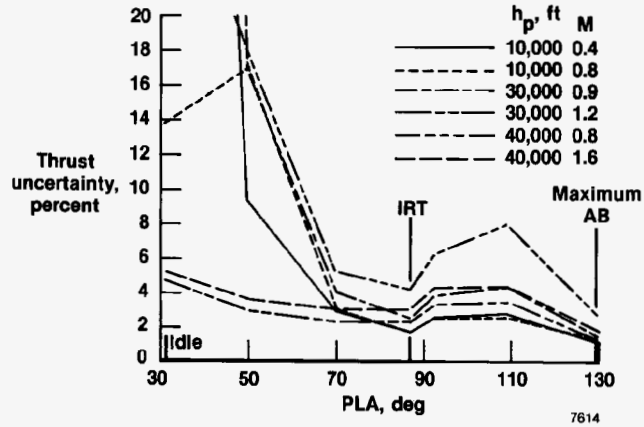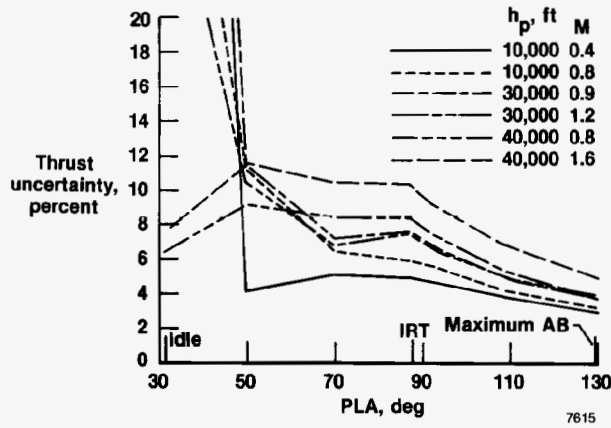

(a) $U_{FG_{WT}}$.
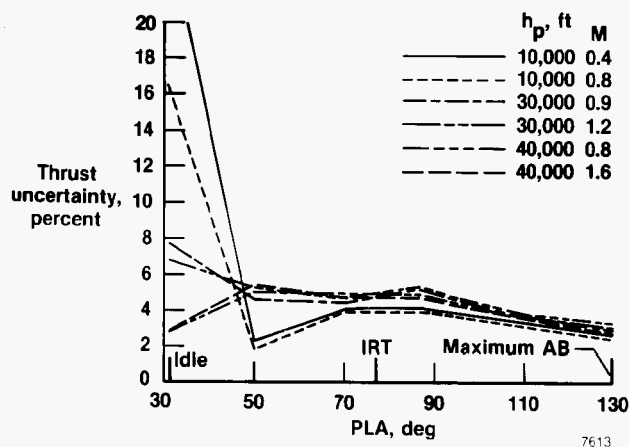
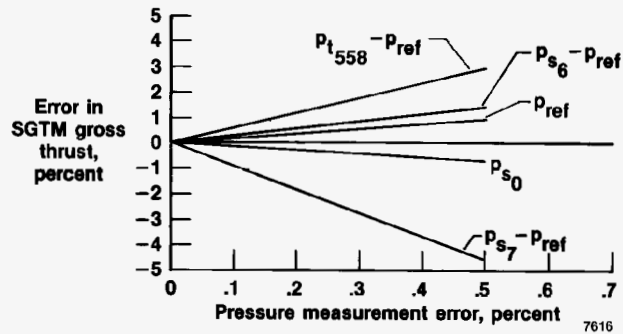(b) $U_{FG_{AP}}$.

Figure 7. Uncertainty in gross and net thrust for a range of flight conditions.

(c) $U_{FN_{WT}}$.

(d) $U_{FN_{AP}}$.

Figure 7. Concluded.

(a) PLA = 70°.

Figure 8. Sensitivity of SGTM to input errors. Mach 0.9, 30,000 ft.
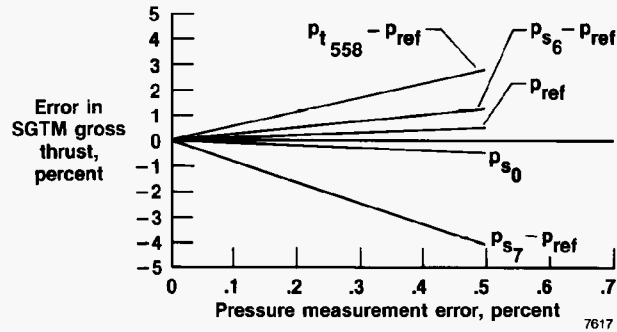
(b) PLA = 87°.
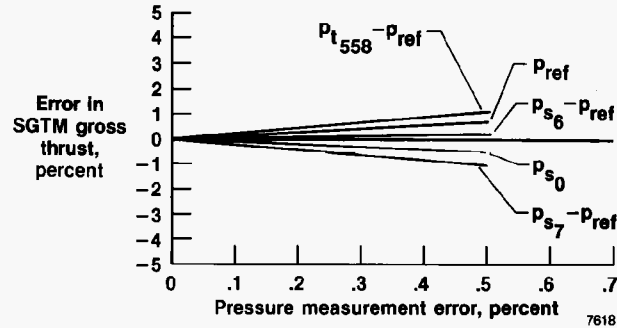
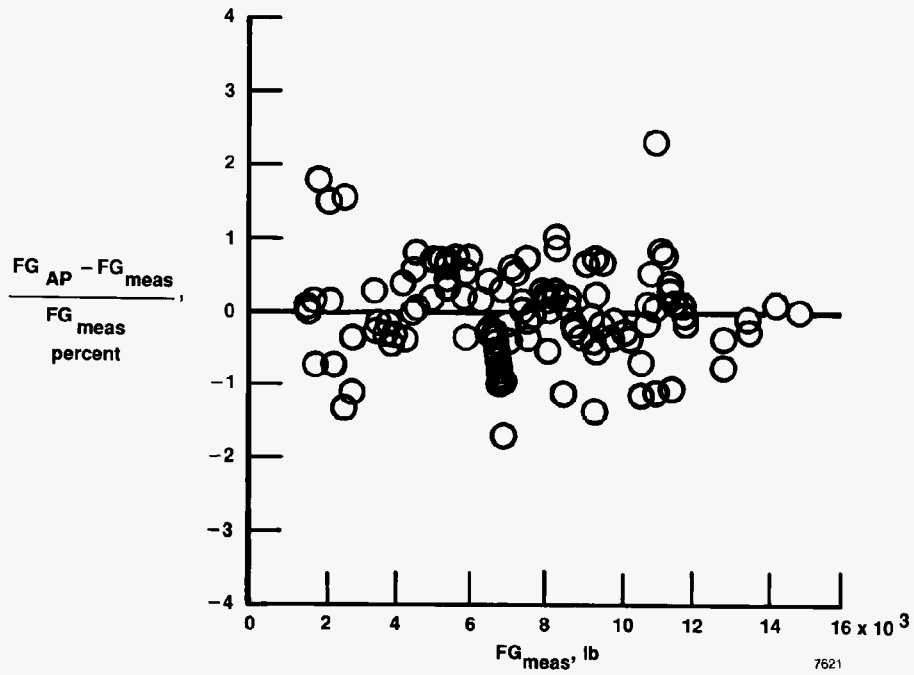(c) PLA = 130°.
Figure 8. Concluded.
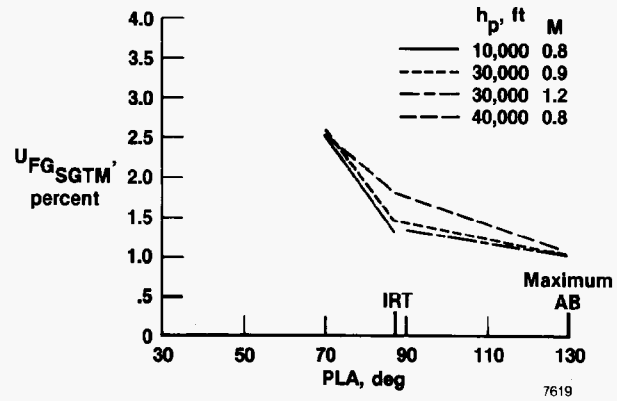
Figure 9. Uncertainty in gross thrust, SGTM.
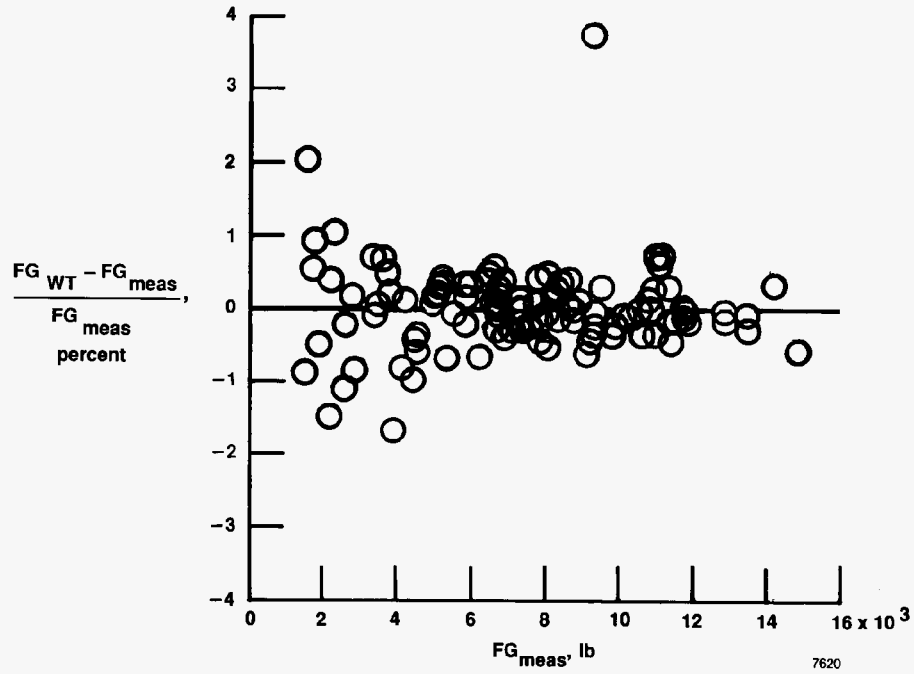
(a) FG_{WT} after calibration.

(b) FG_{AP} after calibration.

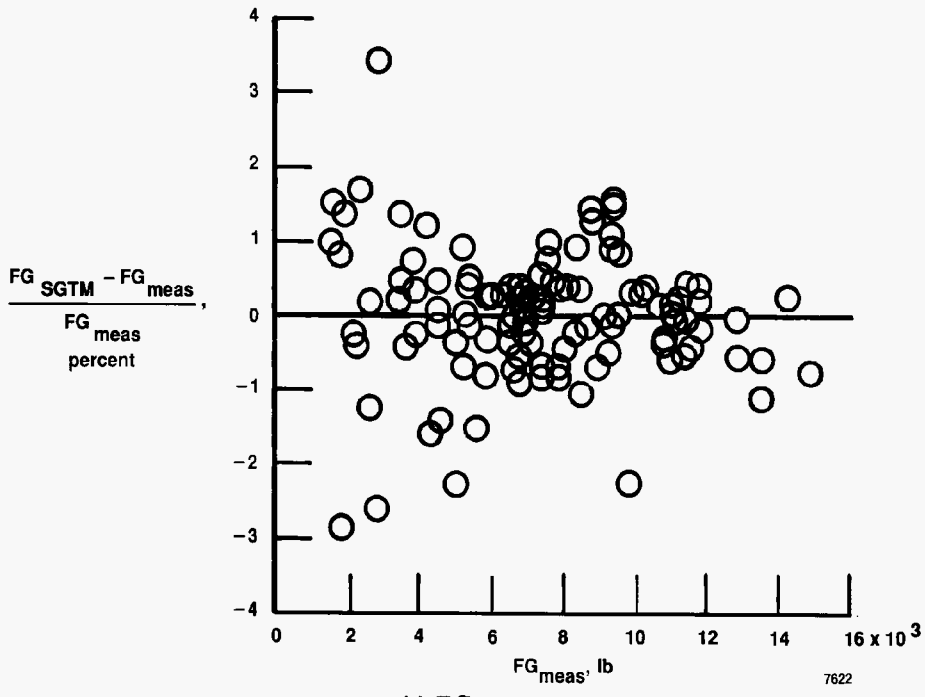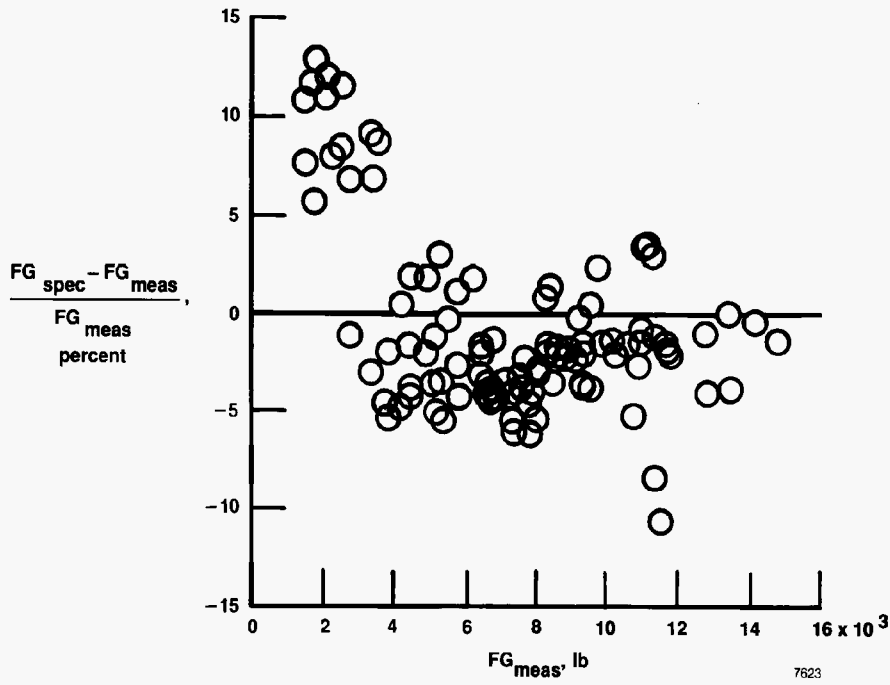Figure 10. Accuracy of the thrust calculation methods after calibration.

(c) FG_{SGTM}.

Figure 10. Concluded.
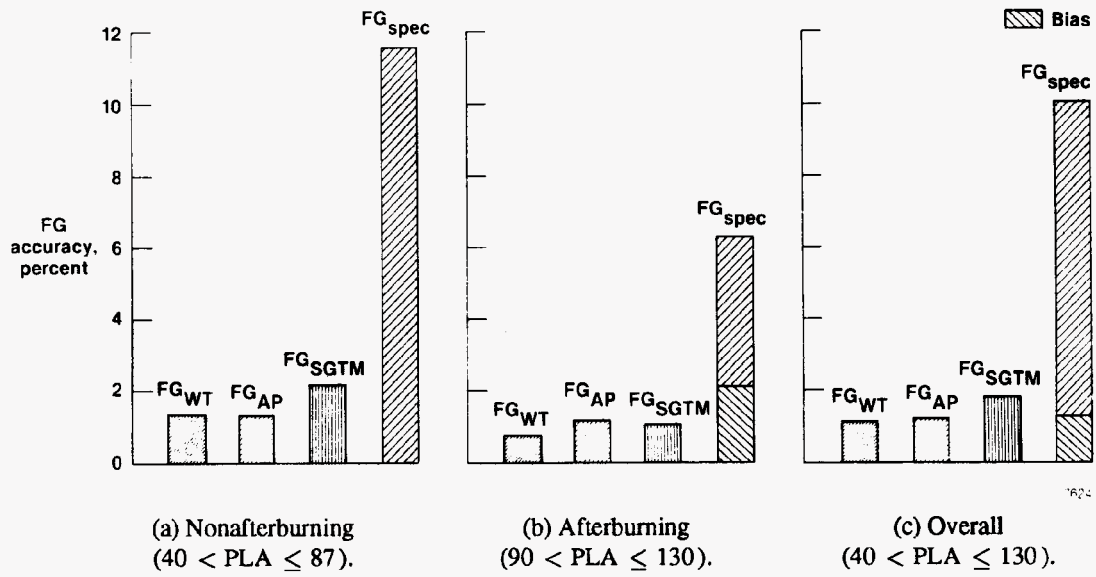

Figure 11. Accuracy of uncalibrated specification gross thrust.

(a) Nonafterburning
$(40 < \text{PLA} \leq 87)$.

(b) Afterburning
$(90 < \text{PLA} \leq 130)$.

(c) Overall
$(40 < \text{PLA} \leq 130)$.

Figure 12. Comparison of $2\,\sigma$ accuracies of the gross thrust methods.
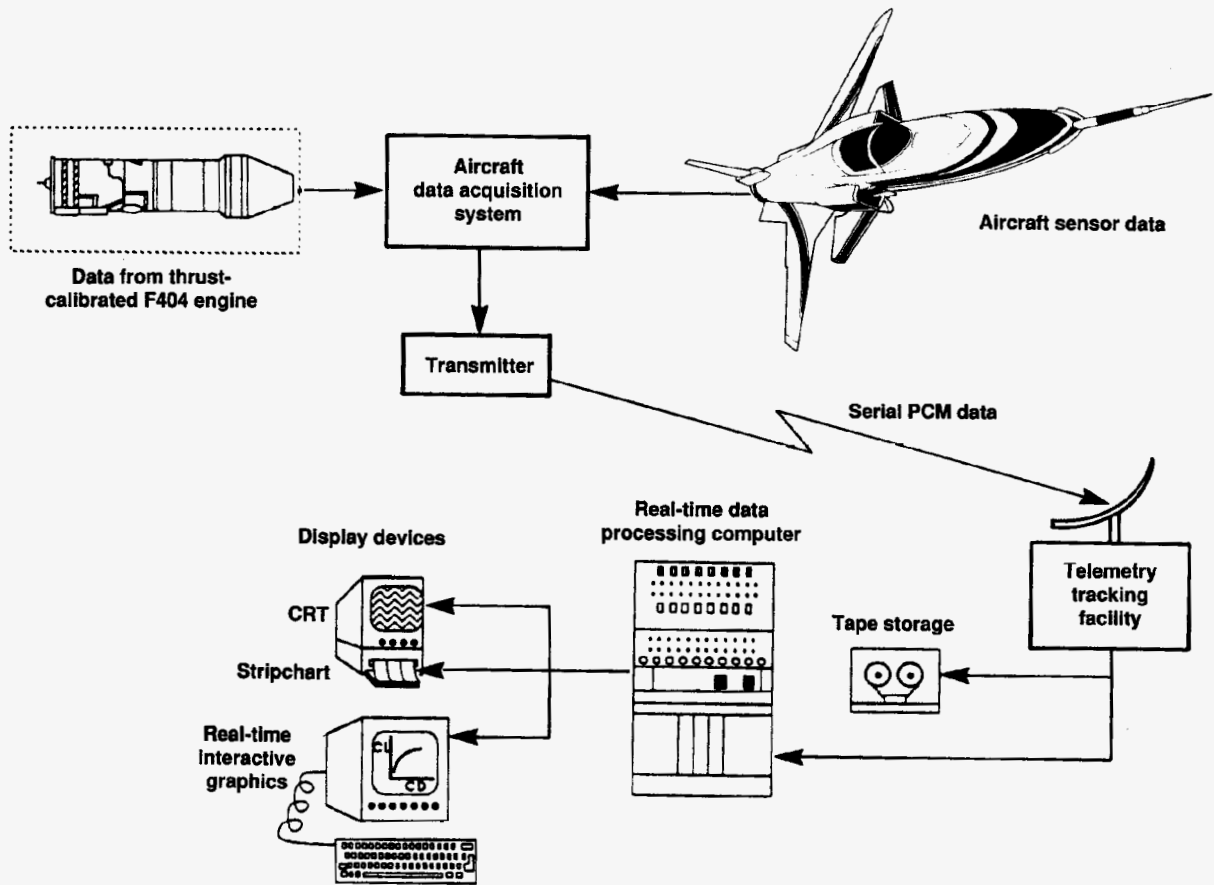
Figure 13. X-29A real-time performance data system.

8144

$$U_{FG_{WT}} + U_{FG_{AP}} = 1.39\% + 3.98\%$$
$$= 5.37\%$$
$$= 563.8 \text{ lb}$$

$$U_{FG_{WT}} + U_{FG_{AP}} = 1.46\% + 4.13\%$$
$$= 5.59\%$$
$$= 475.0 \text{ lb}$$

(a) IRT, 10,000 ft.

7625

$$U_{FG_{WT}} + U_{FG_{AP}} = 1.04\% + 2.81\%$$
$$= 3.85\%$$
$$= 500.9 \text{ lb}$$
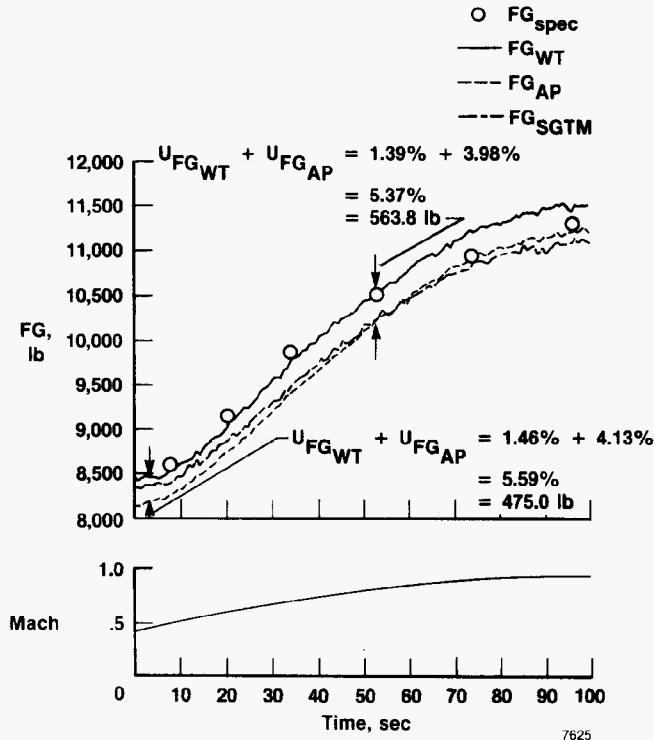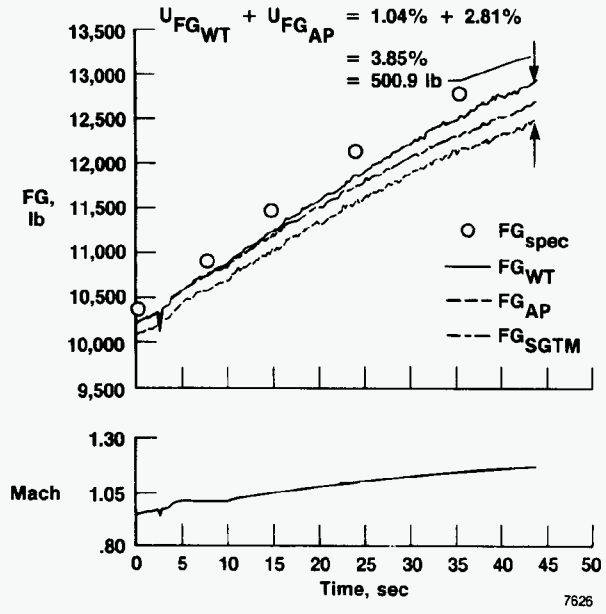
(b) Maximum power, 30,000 ft.

7626

Figure 14. Comparison of gross thrust methods during level accelerations.

26

Report Documentation Page

1. Report No. NASA TP-3001	2. Government Accession No.	3. Recipient's Catalog No.

4. Title and Subtitle	5. Report Date
Evaluation of Various Thrust Calibration Techniques on an F404 Engine	April 1990
	6. Performing Organization Code

7. Author(s)	8. Performing Organization Report No.
Ronald J. Ray	H-1505
	10. Work Unit No. RTOP 533-02-51

9. Performing Organization Name and Address	11. Contract or Grant No.
NASA Ames Research Center Dryden Flight Research Facility P.O. Box 273, Edwards, CA 93523-0273	
	13. Type of Report and Period Covered Technical Paper

12. Sponsoring Agency Name and Address	14. Sponsoring Agency Code
National Aeronautics and Space Administration Washington, DC 20546	

15. Supplementary Notes

16. Abstract

In support of performance testing of the X-29A aircraft at the NASA Ames Research Center, Dryden Flight Research Facility, various thrust calculation techniques have been developed and evaluated for use on the F404-GE-400 engine. The engine was thrust calibrated at the NASA Lewis Research Center's Propulsion System Laboratory. Results from these tests were used to correct the manufacturer's in-flight thrust program to more accurately calculate thrust for the specific test engine. Data from these tests were also used to develop an independent, simplified thrust calculation technique for real-time thrust calculation. Comparisons were also made to thrust values predicted by the engine specification model. Results indicate uninstalled gross thrust accuracies on the order of 1 to 4 percent for the various in-flight thrust methods. The various thrust calculations are described and their usage, uncertainty, and measured accuracies are explained. In addition, the advantages of a real-time thrust algorithm for flight test use and the importance of an accurate thrust calculation to the aircraft performance analysis are described. Finally, actual data obtained from flight test are presented.

17. Key Words (Suggested by Author(s))	18. Distribution Statement
Calibrated thrust Performance Real-time thrust Thrust	Unclassified — Unlimited Subject category 05

19. Security Classif. (of this report)	20. Security Classif. (of this page)	21. No. of pages	22. Price
Unclassified	Unclassified	30	A03

NASA FORM 1626 OCT 86

For sale by the National Technical Information Service, Springfield, VA 22161-2171.